Surface phase transitions in one-dimensional channels arranged in a triangular cross-sectional structure: Theory and Monte Carlo simulations

P. M. Pasinetti
Departamento de Física, Universidad Nacional de San Luis, CONICET, Chacabuco 917, 5700 San Luis, Argentina

F. Romá
Departamento de Física, Universidad Nacional de San Luis, CONICET, Chacabuco 917, 5700 San Luis, Argentina and Centro Atómico Bariloche, CONICET, Avenida Bustillo 9500, 8400 S. C. de Bariloche, Argentina

J. L. Riccardo and A. J. Ramirez-Pastor[a)]
Departamento de Física, Universidad Nacional de San Luis, CONICET, Chacabuco 917, 5700 San Luis, Argentina

(Received 30 June 2006; accepted 20 October 2006; published online 4 December 2006)

Monte Carlo simulations and finite-size scaling analysis have been carried out to study the critical behavior in a submonolayer lattice-gas of interacting monomers adsorbed on one-dimensional channels arranged in a triangular cross-sectional structure. Two kinds of lateral interaction energies have been considered: (1) w_L, interaction energy between nearest-neighbor particles adsorbed along a single channel and (2) w_T, interaction energy between particles adsorbed across nearest-neighbor channels. We focus on the case of repulsive transverse interactions ($w_T>0$), where a rich variety of structural orderings are observed in the adlayer, depending on the value of the parameters k_BT/w_T (being k_B the Boltzmann constant) and w_L/w_T. For $w_L/w_T=0$, successive planes are uncorrelated, the system is equivalent to the triangular lattice, and the well-known $(\sqrt{3}\times\sqrt{3})$ $[(\sqrt{3}\times\sqrt{3})^*]$ ordered phase is found at low temperatures and a coverage, θ, of 1/3 [2/3]. In the more general case ($w_L/w_T\neq 0$), a competition between interactions along a single channel and a transverse coupling between sites in neighboring channels leads to a three-dimensional adsorbed layer. Consequently, the $(\sqrt{3}\times\sqrt{3})$ and $(\sqrt{3}\times\sqrt{3})^*$ structures "propagate" along the channels and new ordered phases appear in the adlayer. Each ordered phase is separated from the disordered state by a continuous order-disorder phase transition occurring at a critical temperature, T_c, which presents an interesting dependence with w_L/w_T. The Monte Carlo technique was combined with the recently reported free energy minimization criterion approach (FEMCA) [F. Romá *et al.*, Phys. Rev. B **68**, 205407 (2003)] to predict the critical temperatures of the order-disorder transformation. The excellent qualitative agreement between simulated data and FEMCA results allows us to interpret the physical meaning of the mechanisms underlying the observed transitions. © *2006 American Institute of Physics*. [DOI: 10.1063/1.2397682]

I. INTRODUCTION

Lattice-gas models have been extensively investigated in the last decades because they provide a theoretical framework for the description of many physical, chemical, and biological systems. The adsorption thermodynamics and the understanding of surface phenomena have been greatly benefited from the development of these models.[1–3] In this sense, the more recognized examples are the Langmuir adsorption model[2,4] and the Ising model of magnetism.[2,5–8] More recently, a number of contributions have been devoted to the study of adsorption of gases on solid surface.[9–22] These papers have included the effects of lateral interactions,[9–13] surface heterogeneity,[14] multisite occupation,[11,15–22] etc. Among them, Phares *et al.*[11] have studied the structural orderings occurring in a wide variety of experimental and theoretical systems and its influence on the corresponding phase diagrams.

Recently, the advent of modern techniques for building single and multiwalled carbon nanotubes[23–27] has considerably encouraged the investigation of the gas-solid interaction (adsorption and transport of simple and polyatomic adsorbates) in such a low-dimensional confining adsorption potentials. The design of carbon tubules, as well as of synthetic zeolites and aluminophosphates such as $AlPO_4-5$ (Refs. 28 and 29) having narrow channels, literally provides a way to the experimental realization of quasi-one-dimensional adsorbents. Many studies on conductivity, electronic structure, mechanical strength, etc., of carbon nanotubes are being cur-

[a)]Author to whom correspondence should be addressed. Electronic mail: antorami@unsl.edu.ar

rently carried out. However, the amount of theoretical and experimental works done on the interaction and thermodynamics of simple gases adsorbed in nanotubes is still limited.

A problem of considerable importance in adsorption is that of determining where on the nanotube bundles the gas molecules adsorb.[30–43] Theoretically there are three possible groups of adsorption sites on bundles of close-ended single-walled carbon nanotubes: (1) interstitial channels formed between the tubes, (2) grooves formed between two adjacent tubes on the bundle surfaces, and (3) exterior surface of individual tubes.[31] For open-ended tubes, a fourth group of adsorption sites can be identified in the interior of individual tubes.[31] Access to each group of adsorption sites is determined by the size of the adsorbate, the size of the nanotubes forming the bundles, the degree of homogeneity of the bundles, and the presence or absence of chemical compounds blocking access to the sites.[31,44–46]

Numerous experimental and theoretical studies of gas adsorption on nanotube bundles suggest that the admolecules form one-dimensional (1D) systems or lines when adsorb within interstitial channels,[36,37] inside nanotubes,[36,38,39] or along the groove sites.[40–42] For theoretical purposes, adsorption in these lines can be treated in the one-dimensional lattice-gas approach.[19,12] This is, of course, an approximation to the state of real adsorbata in nanotubes, which is justified because thermodynamics and transport coefficient can be analytically resolved in these conditions. An example of this kind of models is presented in Refs. 38 and 39. The authors proposed a simple model for adsorption inside a nanotube. That is a lattice-gas model with two kinds of sites. One was a one-dimensional line of sites, which the authors called axial sites, surrounded by a set of cylindrical shell sites. By using mean-field theoretical approach[38] and Monte Carlo (MC) simulations,[39] a rich phase behavior was obtained for attractive or repulsive character of the interspecies interaction.

The influence of transverse interactions between adjacent lines was also studied in the case of adsorption in interstitial channels.[47] In Ref. 47, Cole *et al.* presented a localized anisotropic lattice-gas model with lateral interactions between neighboring atoms within the same channel and attractive transverse interaction between neighbor interstitial channels (arranged in a honeycomb lattice). While the strictly 1D system does not exhibit critical behavior, a phase transition occurs in the system with interacting channels. This phase transition is a condensation of the anisotropic fluid, with droplets extending into contiguous channels.

On the other hand, recent experiments of ^{4}He adsorbed on bundles of single-walled carbon nanotubes[41] shown the existence of different adsorption regimes. At low coverages, single and three 1D chains are formed along the grooves on the bundle surfaces. As the coverage is increased, the admolecules form a two-dimensional (2D) monolayer over the surface of the nanotube bundle thus exhibiting 1D to 2D crossover. Similar behavior has been observed in other systems where the adsorption occurs on the external surface of the nanotube bundle.[43] The existence of close parallel 1D lines of adsorbed atoms suggests the possibility of transverse interactions between neighbor lines.

As discussed in the previous paragraphs, regardless the adsorption taking place in the interior of a nanotube, in interstitial channels or in the groove sites, the interaction between molecules in adjacent chains is essential to the formation of ordered phases at low temperatures. Then, it is of interest and of value to inquire how the transverse interaction between 1D chains influences the phase behavior of the adlayer. It is clear that a complete analysis of this field is a quiet difficult subject. For this reason, the understanding of simple models with increasing complexity might be a help and a guide to establish a general framework for the study of this kind of systems. The present work represents an effort in that direction.

Here, we study a simplified lattice-gas model, which mimics a nanoporous environment. In this model, 1D chains of atoms were arranged in a triangular structure. We included longitudinal interactions between nearest-neighbor particles adsorbed along a single channel, w_L, and transverse energy between particles adsorbed across nearest-neighbor channels, w_T.[48] The phase behavior depends on the values of these various energies. In fact, for $w_T=0$ and $w_L\neq 0$, the adlayer behaves as a one-dimensional fluid, the model is exactly soluble, and no phase transition develops when short-ranged coupling between neighboring particles exists.[49–51] For $w_T \neq 0$ and $w_L=0$, successive transverse planes are uncorrelated and the system is equivalent to the well-known two-dimensional triangular lattice. In this case, the phase diagram has been widely studied for both attractive[52,53] and repulsive nearest-neighbor interactions.[52–55] In the more general case ($w_T\neq 0$ and $w_L\neq 0$), a competition between interactions along a single channel (w_L) and a transverse coupling between sites in neighboring channels (w_T) allows to evolve to a three-dimensional adsorbed layer. Although most of the works on the three-dimensional lattice gas have been devoted to attractive lateral interactions (see, for instance, Refs. 56–59), there have been a few studies related to repulsive couplings between adatoms.

In previous work, low temperature calculations of configurational entropy of the adlayer allowed us to identify a wide variety of structural orderings.[60] Later, the influence of such structural orderings on interesting properties as adsorption isotherm and heat of adsorption was analyzed.[61] The present article goes a step further, studying the critical behavior of the system via MC simulation, finite-size scaling analysis, and the recently reported free energy minimization criterion approach (FEMCA).[22] For this purpose, the critical temperature T_c characterizing the transition from the disordered state to the ordered phase is obtained as a function of the ratio w_L/w_T.

The paper is organized as follows: In Sec. II we describe the lattice-gas model, the simulation scheme, and we present the behavior of $T_c(w_L/w_T)$, obtained by using MC method. In Sec. III we present the theoretical approach (FEMCA) and compare the MC results with the theoretical calculations. Finally, the general conclusions are given in Sec. IV.

II. LATTICE-GAS MODEL AND MONTE CARLO SIMULATION SCHEME

A. The model

As it was discussed in the previous section, numerous experimental and theoretical studies of gas adsorption on carbon nanotube bundles predict the existence of close parallel channels of adatoms when the adsorption takes place (1) in the interior of a nanotube, (2) in interstitial channels, or (3) in the grooves site on bundle surfaces. In this context, we present a simplified lattice-gas model, where each channel or unit cell has been represented by a one-dimensional line of L adsorptive sites, with periodical boundary conditions. In order to include transverse interactions between parallel neighbor lines, these chains were arranged in a triangular structure of size $R \times R$ and periodical boundary conditions. Under these conditions all lattice sites are equivalent hence border effects will not enter our derivation. The energies involved in the adsorption process are three:

(1) ε_0, interaction energy between a particle and a lattice site;
(2) w_L, interaction energy between adjacent occupied axial sites; and
(3) w_T, interaction energy between particles adsorbed on nearest-neighbor transverse sites.

Thus, the resulting substrate was an anisotropic three-dimensional array of $M=L\times R\times R$ adsorption sites, where each site was surrounded by two "axial" sites along chain's axis and six "transverse" sites belonging to nearest-neighbor unit cells (see Fig. 1 in Ref. 60).

In order to describe the system of N molecules adsorbed on M sites at a given temperature T, let us introduce the occupation variable $c_{i,j,k}$ which can take the following values: $c_{i,j,k}=0$ if the corresponding site (i,j,k) is empty and $c_{i,j,k}=1$ if the site is occupied by an adatom. Then, the Hamiltonian of the system is given by

$$H = w_L \sum_{\langle i,j,k;i',j',k'\rangle_L} c_{i,j,k}c_{i',j',k'} + w_T \sum_{\langle i,j,k;i',j',k'\rangle_T} c_{i,j,k}c_{i',j',k'} + (\varepsilon_0 - \mu)\sum_{i,j,k}^{M} c_{i,j,k}, \quad (1)$$

where $\langle i,j,k;i',j',k'\rangle_L$ ($\langle i,j,k;i',j',k'\rangle_T$) represents pairs of NN axial (transverse) sites and μ is the chemical potential.

B. Monte Carlo simulations

The lattice gas was generated fulfilling the following conditions:

- The sites were arranged in a structure of size $M=L\times R\times R$, with conventional periodic boundary conditions.
- Due to the surface was assumed to be homogeneous, the interaction energy between the adparticles and the atoms of the substrate, ε_0, was neglected for sake of simplicity.
- Repulsive transverse lateral interactions were considered, where a rich variety of ordered phases are observed in the planes. Although, repulsive transverse interaction between adjacent channels may not resemble a particular experimental realization, this case has intrinsically theoretical interest. However, it is worth mentioning that adsorption of polar molecules could eventually result in either repulsive or attractive long range transverse interactions considering that the confining geometry of the tubes, grooves, or interstitial channels represents a major constraint to the spatial orientation of the admolecule.
- Repulsive and attractive longitudinal lateral interactions were used.
- Appropriate values of L and R were used in such a way that the adlayer structures at critical regime are not perturbed.

In order to study the critical behavior of the system, we have used an efficient exchange MC or simulated tempering method[62,63] and finite-size scaling analysis.[64–66] As in Ref. 62, we build a compound system which consists of m noninteracting replicas of the system concerned. The mth replica is associated with the temperature T_m [or $\beta_m=1/(k_B T_m)$, being k_B the Boltzmann constant]. In other words, each replica is in contact with its own heat bath having different temperatures. Under these conditions, the algorithm to carry out the simulation process is the following.

(1) The compound system of m replicas is generated. For this purpose, each replica is simulated simultaneously and independently as canonical ensemble for n_1 MC steps by using a standard importance sampling MC method.[66–68] In order to determine the set of temperatures, $\{T_m\}$ ($\{\beta_m\}$), we set the highest temperature, $T_{\max}$ ($\beta_{\min}$), in the high temperature phase where relaxation (correlation) time is expected to be very short and there exists only one minimum in the free energy space. On the other hand, the lowest temperature, $T_{\min}$ ($\beta_{\max}$), is somewhere in the low temperature phase whose properties we are interested in. Finally, the difference between two consecutive temperatures is set as $(T_{\max}-T_{\min})/(m-1)$ (equally spaced temperatures).
(2) Interchange vacancy particle. The procedure is as follows.
  (i) One of the m replicas is randomly selected.
  (ii) An occupied site and an empty site, both belonging to the replica chosen in (i), are randomly selected and their positions are established.
  (iii) By using a standard Kawasaki algorithm,[69] an attempt is made to interchange the occupancy state of the sites chosen in step (ii).
(3) Exchange of two configurations X_m and $X_{m'}$, corresponding to the mth and m'th replicas, is tried and accepted with the probability $W(X_m,\beta_m|X_{m'},\beta_{m'})$. In general, the probability of exchanging configurations of the mth and m'th replicas is given by[62]

$$W(X_m,\beta_m|X_{m'},\beta_{m'}) = \begin{cases} 1 & \text{for } \Delta < 0 \\ \exp(-\Delta) & \text{for } \Delta > 0, \end{cases} \quad (2)$$

where $\Delta=(\beta_m-\beta_{m'})[H(X_{m'})-H(X_m)]$. As in Ref. 62, we restrict the replica exchange to the case $m \leftrightarrow m+1$.

(4) Repeat from step (2) $m \times M$ times. This is the elementary step in the simulation process or Monte Carlo step (MCS).

The procedures (1)–(4) are repeated for all lattice's sizes. For each size, the equilibrium state can be well reproduced after discarding the first n_2 MCS. Then, averages are taken over n_{MCS} successive MCS. The canonical expectation value of a physical quantity A is obtained in the usual way as follows:

$$\langle A\rangle_{\beta_m} = \frac{1}{n_{\mathrm{MCS}}} \sum_{t=1}^{n_{\mathrm{MCS}}} A[X_m(t)] \quad (3)$$

All calculations were carried out using the parallel cluster BACO of Universidad Nacional de San Luis, Argentina. This facility consists of 60 personal computers (PCs) each with a 3.0 GHz Pentium-4 processor.

As it is standard for order-disorder phase transitions, a related order parameter was defined. In particular, at $\theta=1/3$ [2/3] (being $\theta \equiv N/M$ the surface coverage), a $(\sqrt{3}\times\sqrt{3})$ $[(\sqrt{3}\times\sqrt{3})^*]$ ordered structure is formed in the planes below the critical temperature. Depending on the sign of the longitudinal interactions, the order is propagated to all planes. For repulsive w_L, adatoms avoiding configurations with nearest-neighbor interactions order along the channels in a structure of alternating particles separated by empty sites. On the other hand, attractive monomer-monomer longitudinal interactions favor the formation of pairs of nearest-neighbor adsorbed particles along the lines. The resulting structures are shown in Figs. 5 and 8 of Ref. 60.

For the case of repulsive longitudinal interactions, Fig. 1(a) shows two successive planes, k and $k+1$, for one possible configuration of the phase appearing at critical regime and $\theta=1/3$. Due to the periodic boundary conditions the degeneracy of this "local phase" is equal to 6. These configurations allow us to decompose the "local lattice" into six different sublattices [see Figs. 1(b) and 1(c)].[70] The coverage on each sublattice is denoted as $\theta_s(s=1,\ldots,6)$. In this way, a "local order parameter," φ_k, can be defined as

$$\varphi_k = \sum_{s,t;s\neq t} |\theta_s - \theta_t|, \quad (4)$$

where we sum the differences (in absolute value) between the coverage corresponding to two sublattices.

When the system is disordered $(T>T_c)$, all sublattices are equivalents and the order parameter is minimum. However, when a configuration of the local phase appears at low temperature $(T<T_c)$, this is allocated on a sublattice. Let us suppose that this configuration lies on the sublattice s. Then, the coverage θ_s is maximum $(\theta_s=1)$ and the coverage of the rest of the sublattices is zero or minimum. Consequently, φ_k is also maximum.

On the basis of φ_k, the generalized order parameter, φ, can be written as

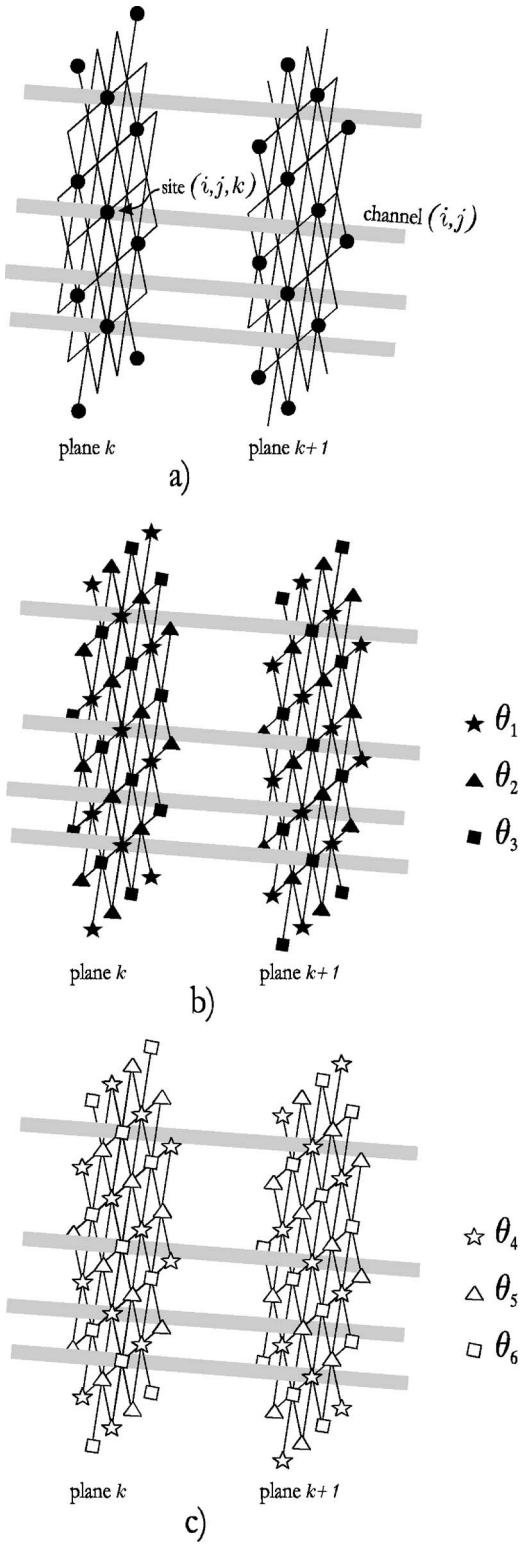

FIG. 1. (a) Snapshot of two successive planes, k and $k+1$, for a possible configuration of the ordered phase appearing at $\theta=1/3$ and repulsive longitudinal interactions. The solid circles represent occupied sites. The different sublattices used in order to define a local order parameter characterizing this low temperature structure are shown in parts (b) and (c).

$$\varphi = A\sum_{k=0}^{L} \varphi_k, \quad (5)$$

where A is a normalization factor. The definition (5) is computationally convenient and φ appears as a good order pa-

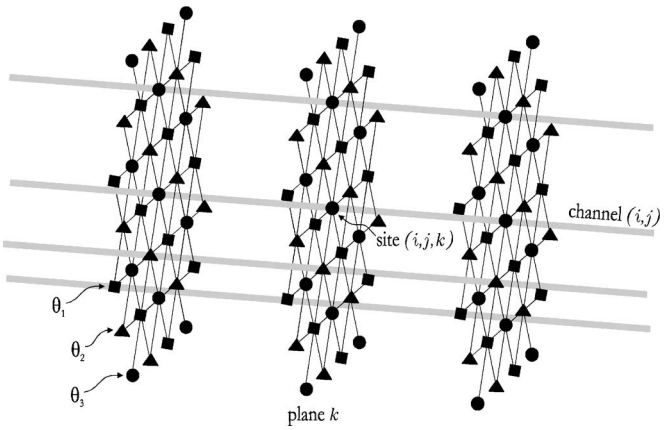

FIG. 2. Different sublattices defined for attractive longitudinal interactions and $\theta=1/3$.

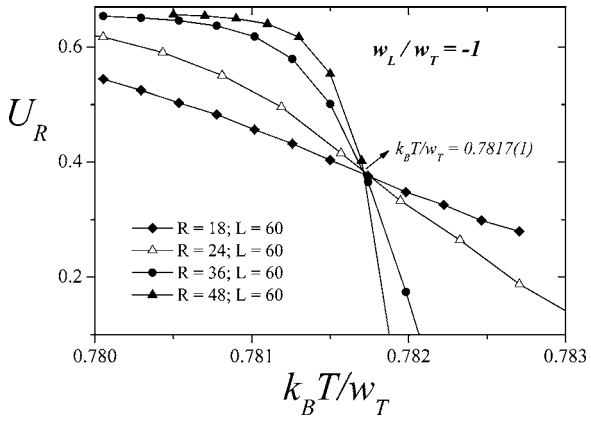

FIG. 3. $U_R(T)$ and $U_L(T)$ (inset) vs k_BT/w_T, for a typical case of $w_L<0$: $\theta=1/3$ and $w_L/w_T=-1$.

rameter evidencing the order-disorder phase transition.

In a similar way, it is possible to define the order parameter corresponding to $\theta=2/3$ and repulsive longitudinal interactions.

For attractive longitudinal interactions, it is not appropriate to define local sublattices. In this case, each sublattice $s(s=1,\ldots,3)$ lies on the total lattice (see Fig. 2) and φ can be easily defined as $\varphi=|\theta_1-\theta_2|+|\theta_1-\theta_3|+|\theta_2-\theta_3|$.

Now, the reduced fourth-order cumulant, $U_{R[L]}$, introduced by Binder[66] and related to the order parameter, can be calculated as

$$U_{R[L]}(T)=1-\frac{\langle\varphi^4\rangle_T}{3\langle\varphi^2\rangle_T^2}, \tag{6}$$

where U_R $[U_L]$ represents the cumulant obtained by variable R $[L]$ and fixed L $[R]$. The thermal average $\langle\ldots\rangle_T$, in all the quantities, means the time average throughout the MC simulation.

The standard theory of finite-size scaling[64–66] allows for various efficient routes to estimate T_c from MC data. One of these methods, which will be used here, is from the temperature dependence of $U_{R[L]}(T)$, which is independent of the system size for $T=T_c$. In other words, T_c is found from the intersection of the curve $U_{R[L]}(T)$ for different values of R $[L]$, since $U_{R[L]}(T_c)=\text{const}$.

C. Computational results

The thermodynamic properties of the present model have been investigated by means of the computational scheme described in the previous section. As a consequence of the equivalence particle vacancy, the critical behavior at $\theta=2/3$ is as at $\theta=1/3$. Then, we restrict our calculations to $\theta=1/3$. In addition, we set $w_T=1$ and vary w_L/w_T from -1 to 1 $(-1\leqslant w_L/w_T\leqslant 1)$.

In order to understand the basic phenomenology, we consider in the first place null longitudinal interactions $(w_L/w_T=0)$. In this particular case, successive planes are uncorrelated and the system is equivalent to the well-known triangular lattice. The value obtained of $k_BT_c/w_T=0.3354(1)$ confirms this arguments and validates the MC scheme.[71–74] The data are not shown here for brevity.

Hereafter, we discuss the behavior of the critical temperature as a function of w_L/w_T. We start with the case of attractive longitudinal interactions. As an example, Fig. 3 illustrates the reduced four-order cumulants plotted versus k_BT/w_T for $w_L/w_T=-1$. From their intersections one gets the estimation of the critical temperature. The lattice sizes used in the simulation[75] are compiled in Table I along with the values of the parameters in the simulated tempering runs. In the figure, the critical temperature is obtained from the curves of $U_R(T)$ (calculated for different values of R and fixed L). The resulting value, $k_BT_c/w_T=0.7817(1)$, agrees very well with previous determinations reported in the literature.[60] In Ref. 60, a value $k_BT_c/w_T\approx 0.76$ was obtained

TABLE I. Parameters of the simulated tempering runs for two typical cases $(w_L/w_T=-1,1)$.

w_L/w_T	R	L	m	n_1	n_2	n_{MCS}	$k_BT_{\min}/w_T$	$k_BT_{\max}/w_T$
−1	18	60	12	10^3	10^5	10^5	0.780 053	0.782 705
	24	60	20	10^3	10^5	10^5	0.777 400	0.784 600
	36	60	12	10^3	10^5	10^5	0.780 053	0.782 705
	48	60	11	10^3	10^5	10^5	0.780 500	0.782 500
1	18	60	12	10^3	5.10^5	5.10^5	0.601 053	0.617 632
	24	60	12	10^3	5.10^5	5.10^5	0.601 053	0.617 632
	36	60	12	10^3	5.10^5	5.10^5	0.601 053	0.617 632
	48	60	12	10^3	5.10^5	5.10^5	0.601 053	0.617 632

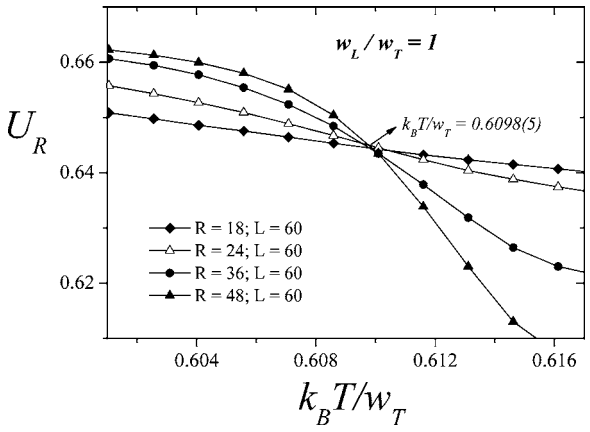

FIG. 4. $U_R(T)$ vs k_BT/w_T for $\theta=1/3$ and $w_L/w_T=1$.

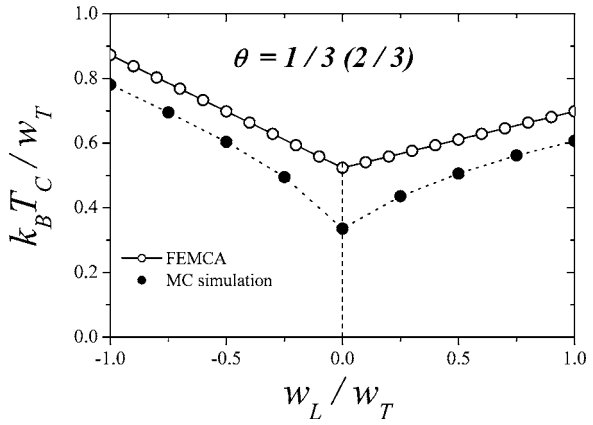

FIG. 6. Comparison between simulated and theoretical results for k_BT_c/w_T vs w_L/w_T at $\theta=1/3(2/3)$. The dotted lines are a guide for the eyes.

from the inflection on the function $s(T)$, being $s(T)$ the configurational entropy per site of the adlayer as a function of the temperature. Due to the finite-size scaling technique and the simulation procedure used in this contribution, the estimation of T_c in the present work is expected to be more accurate than that reported previously.

The study was extended to repulsive longitudinal interactions. Figure 4 shows the data for a typical case ($w_L/w_T=1$), resulting $k_BT_c/w_T=0.6098(5)$, in well agreement with the value obtained in Ref. 60 ($k_BT_c/w_T\approx 0.59$). As indicated in Fig. 3, the parameters of the simulation are listed in Table I.

Due to the presence of anisotropy (the couplings are taken to be different in the different lattice directions), it is expected that the correlation functions in transverse and longitudinal directions may be governed by correlation lengths diverging with different critical exponents.[76,77] However, it is worth pointing out that we do not assume any particular value of the critical exponents for the transitions analyzed here in order to calculate their critical temperatures, since the analysis rely on order parameter cumulant's properties.[78] In addition, the procedure shown in Figs. 4 and 5 was repeated for the curves of $U_L(T)$, which were obtained for variable L and fixed R. As an example, Fig. 6 presents the results obtained for the case $w_L/w_T=-1$. As it is expected, identical results (within numerical errors) are obtained in both ways.

Finally, the calculations were carried out for $w_L/w_T=$ -0.75, -0.50, -0.25, 0.00, 0.25, 0.50, and 0.75 and the results were collected in Table II.[79] As it can be observed, the critical temperature presents a nontrivial behavior as a function of w_L/w_T. An understanding of the dependence of k_BT_c/w_T on w_L/w_T can be developed by following the subtle interdependence of energetic and entropic costs necessary to alter the ordered phase. This will be discussed in Sec. III.

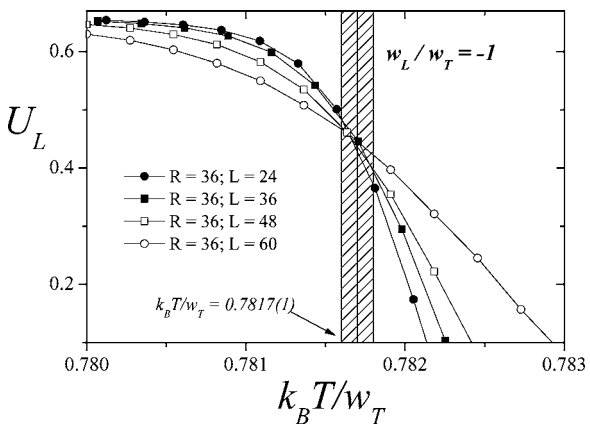

FIG. 5. $U_L(T)$ vs k_BT/w_T for $\theta=1/3$ and $w_L/w_T=-1$.

III. THEORETICAL APPROACH: FREE ENERGY MINIMIZATION CRITERION

Hereafter, we will use FEMCA (Ref. 22) in order to discuss the dependence of k_BT_c/w_T vs w_L/w_T obtained from MC simulation.

In a closed system of adsorbed particles with repulsive interactions, the phase transition occurring in the adsorbate is a continuous (second-order) phase transition. In other words, the entropy, S, varies continuously from a completely ordered state (when $T\to 0$) to a disordered state (when $T\to\infty$). Around T_c, S changes abruptly (but continuously).[21] Then, it is possible to analyze the phase transition taking into account the Helmholtz free energy, $F=E-TS$ (being E the mean energy), in the two extreme states (maximum order and maximum disorder). Accordingly,

$$F_\infty = \lim_{T\to\infty} F \text{ and } F_0 = \lim_{T\to 0} F, \tag{7}$$

then

TABLE II. Critical temperatures corresponding to the critical coverage $\theta=1/3(2/3)$. The data were obtained from the crossing of the cumulants.

w_L/w_T	k_BT_c/w_T $\theta=1/3(2/3)$
−1.00	0.7817(1)
−0.75	0.695(4)
−0.50	0.604(4)
−0.25	0.495(4)
0.00	0.3354(1)
0.25	0.436(1)
0.50	0.506(1)
0.75	0.562(1)
1.00	0.6098(5)

$$F_\infty \ll F_0 \Rightarrow T > T_c, \tag{8}$$

$$F_\infty \gg F_0 \Rightarrow T < T_c, \tag{9}$$

$$F_\infty = F_0 \Rightarrow T \approx T_c. \tag{10}$$

The last equation allows to determine T_c. This calculation is not exact due to the system that does not pass from an extreme order to an extreme disorder. There exist intermediate states between the two extreme states. However, as we will show in the following analysis, Eq. (10) provides a very good approximation for T_c. Interested readers are referred to Ref. 22 for a more complete description of FEMCA.

In general, for a system of interacting particles at temperature T results

$$f_0 = e_0 - Ts_0 \text{ and } f_\infty = e_\infty - Ts_\infty \tag{11}$$

where e and s represent the mean energy per site and the entropy per site in the thermodynamical limit, respectively,

$$e = \lim_{M\to\infty} \frac{E}{M} \text{ and } s = \lim_{M\to\infty} \frac{S}{M}. \tag{12}$$

If $f_0 = f_\infty$, this is

$$e_0 - Ts_0 = e_\infty - Ts_\infty, \tag{13}$$

then $T \approx T_c$ and

$$T_c \approx \frac{\Delta e}{\Delta s} = \frac{e_\infty - e_0}{s_\infty - s_0}. \tag{14}$$

From Eq. (14), it is possible to calculate the critical temperature and to interpret the dependence of $k_B T_c/w_T$ with w_L/w_T obtained from simulations. As in Sec. II, we restrict the study to $\theta = 1/3(2/3)$ and $-1 < w_L/w_T < 1$.

Case I: $\theta = 1/3$ and $w_L/w_T > 0$. In general, $e_\infty(\theta)$ can be calculated from mean-field approximation. Thus,

$$e_\infty(\theta) = \frac{1}{2M}(6N\theta w_T + 2N\theta w_L). \tag{15}$$

In this case $\theta = N/M = 1/3$, and

$$e_\infty(1/3) = \tfrac{1}{3}w_T + \tfrac{1}{9}w_L. \tag{16}$$

In order to calculate the entropy of the disordered state, the configurational factor of monomers Ω, is employed

$$\Omega = \frac{M!}{N!(M-N)!}. \tag{17}$$

Thus,

$$s_\infty = \lim_{M\to\infty} \frac{k_B \ln \Omega}{M}. \tag{18}$$

In the particular case of $\theta = 1/3$, the entropy per site of the disordered state results

$$s_\infty(1/3) = -k_B\left(\ln \tfrac{1}{3} + \tfrac{2}{3}\ln 2\right). \tag{19}$$

In addition, the mean energy per site and the entropy per site for the ordered state at $\theta = 1/3$ and $T = 0$ are $e_0(1/3) = s_0(1/3) = 0$. Then, the critical temperature depends on the mean energy and the entropy of the disordered state. From Eqs. (16), (19), and (14), we obtain $T_c(1/3)$:

$$T_c(1/3) \approx \frac{e_\infty(1/3)}{s_\infty(1/3)} \approx \frac{(1/3)w_T + (1/9)w_L}{-k_B(\ln(1/3) + (2/3)\ln 2)}. \tag{20}$$

Finally,

$$\frac{k_B T_c(1/3)}{w_T} \approx \frac{(1/3) + (1/9 w_L/w_T)}{-\ln(1/3) - (2/3)\ln 2} \quad (w_T > 0 \text{ and } w_L/w_T > 0). \tag{21}$$

Case II: $\theta = 1/3$ and $w_L/w_T < 0$. The mean energy and the entropy of the disordered system are as in Eqs. (15) and (18). On the other hand, for the ordered system, $s_0(1/3) = 0$ and $e_0(1/3) = w_L/3$. Then

$$\frac{k_B T_c(1/3)}{w_T} \approx \frac{(1/3) - (2/9 w_L/w_T)}{-\ln(1/3) - (2/3)\ln 2} \quad (w_T > 0 \text{ and } w_L/w_T < 0). \tag{22}$$

As it is expected, the calculations for $\theta = 2/3$ (do not shown here) provide identical results as cases I and II.

Figure 6 shows the comparison between the simulated results previously presented in Table II and the theoretical predictions obtained from FEMCA for the critical temperature as a function of w_L/w_T. The MC simulations reveal the main characteristics for the behavior of the critical temperature versus w_L/w_T: (i) the curve presents a minimum for $w_L/w_T = 0$, and (ii) for negative values of w_L/w_T, the critical temperatures are higher than the corresponding ones for positive w_L/w_T's. Both characteristics are very well reproduce by FEMCA.

The physical meaning of the main features of the critical temperature can be interpreted from the theoretical approach. In this framework, Eq. (14) shows that $k_B T_c/w_T$ depends on the mean energy and the entropy of the disordered state. The behavior of these quantities as a function of w_L/w_T allows to understand the arguments presented in the previous paragraph. Thus, the values of s_∞, s_0, and e_∞ are identical for repulsive and attractive longitudinal interactions. In addition, the magnitude of e_0 is constant ($e_0 = 0$) for $w_L > 0$ and increases with w_L ($e_0 = w_L/3$) for $w_L < 0$. Now we can interpret the difference between the two regimes in Fig. 6. From $-1 < w_L/w_T < 1$, the variation in the entropy is constant. On the other hand, the variation of the mean energy increases linearly with w_L, being higher for $w_L < 0$ than for $w_L > 0$.

IV. CONCLUSIONS

In the present work, we have addressed the critical properties of a simple lattice-gas model, which mimics a nanoporous environment, where each channel or unit cell is represented by a one-dimensional array. The results were obtained by using MC simulations, finite-size scaling theory and the recently reported FEMCA, which is based on a free energy minimization criterion.

The system was characterized by two parameters w_L/w_T and $k_B T/w_T$, being w_L and w_T, the longitudinal and transverse energies, respectively. We focused on the case of re-

pulsive transverse interaction energy among adsorbed particles ($w_T=1$) and $\theta=1/3(2/3)$, in such a way that a rich variety of ordered phases are observed in the adlayer.

- For $w_L/w_T=0$, the system is equivalent to the well-known triangular lattice in 2D.
- For $w_L/w_T<0$, the formation of pairs of nearest-neighbor adsorbed particles along the lines is favored. Consequently, the $(\sqrt{3}\times\sqrt{3})$ and $(\sqrt{3}\times\sqrt{3})^*$ phases are reinforced and extend along the channels. The critical temperature decreases from 0.7817(1) for $w_L/w_T=-1$ to 0.3354(1) for $w_L/w_T=0$.
- For $w_L/w_T>0$, the $(\sqrt{3}\times\sqrt{3})$ and $(\sqrt{3}\times\sqrt{3})^*$ structures are formed in the planes at low temperatures and order along the channels in an array of alternating particles. The critical temperature increases from 0.3354(1) for $w_L/w_T=0$ to 0.6098(5) for $w_L/w_T=1$.

With respect to the analytical approach, FEMCA provides results in very good qualitative agreement with MC simulations and constitutes a theoretical framework in order to interpret the behavior of k_BT_c/w_T vs w_L/w_T in the critical concentrations.

Future efforts will be directed to (a) include attractive w_T longitudinal interactions between the adparticles, (b) obtain the phase diagram k_BT_c/w_T vs θ in the whole range of coverage, and (c) develop an exhaustive study on critical exponents and universality.

ACKNOWLEDGMENTS

This work was supported in part by CONICET (Argentina) under Project No. PIP 6294 and the Universidad Nacional de San Luis (Argentina) under Project Nos. 328501 and 322000. One of the authors (A.J.R.-P.) is grateful to the Departamento de Química, Universidad Autónoma Metropolitana-Iztapalapa (México, D.F.) for its hospitality during the time this manuscript was prepared.

[1] R. H. Fowler and E. A. Guggenheim, *Statistical Thermodynamics* (Cambridge University Press, Cambridge, 1949).
[2] T. L. Hill, *An Introduction to Statistical Thermodynamics* (Addison-Wesley, Reading, MA, 1960).
[3] H. E. Stanley, *Introduction to Phase Transitions and Critical Phenomena* (Oxford University Press, New York, 1971).
[4] I. Langmuir, J. Am. Chem. Soc. **34**, 1310 (1912); **37**, 417 (1951); **54**, 2798 (1932); Gen. Electr. Rev. **29**, 153 (1926); I. Langmuir and K. H. Kingdom, Proc. R. Soc. London, Ser. A **107**, 61 (1925); Phys. Rev. **34**, 129 (1919); I. Langmuir and J. B. Taylor, *ibid.* **44**, 423 (1933); I. Langmuir and D. S. Villars, J. Am. Chem. Soc. **53**, 486 (1931).
[5] E. Ising, Z. Phys. **31**, 253 (1925).
[6] H. A. Kramers and G. H. Wannier, Phys. Rev. **60**, 252 (1941); **60**, 263 (1941).
[7] E. Montroll, J. Chem. Phys. **9**, 706 (1941).
[8] L. Onsager, Phys. Rev. **65**, 117 (1944).
[9] K. Binder and D. P. Landau, Phys. Rev. B **21**, 1941 (1980).
[10] D. P. Landau, Phys. Rev. B **27**, 5604 (1983).
[11] A. J. Phares and F. J. Wunderlich, J. Math. Phys. **26**, 2491 (1985); Phys. Rev. E **52**, 2236 (1995); **55**, 2403 (1997); A. J. Phares and F. J. Wunderlich, Surf. Sci. **425**, 112 (1999); **452**, 108 (2000); **479**, 43 (2001).
[12] F. Romá and A. J. Ramirez-Pastor, Phys. Rev. E **69**, 036124 (2004).
[13] A. Patrykiejew, S. Sokolowski, and K. Binder, Surf. Sci. Rep. **37**, 207 (2000).
[14] F. Bulnes, A. J. Ramirez-Pastor, and G. Zgrablich, J. Chem. Phys. **115**, 1513 (2001); Phys. Rev. E **65**, 31603 (2002).
[15] T. Nitta, M. Kuro-Oka, and K. Katayama, J. Chem. Eng. Jpn. **17**, 45 (1984).
[16] W. Rudzinski, K. Nieszporek, J. M. Cases, L. I. Michot, and F. Villeras, Langmuir **12**, 170 (1996).
[17] M. Borówko and W. Rżysko, J. Colloid Interface Sci. **182** 268 (1996); Ber. Bunsenges. Phys. Chem. **101**, 84 (1997).
[18] W. Rżysko and M. Borówko, J. Chem. Phys. **117**, 4526 (2002); Surf. Sci. **520**, 151 (2002).
[19] A. J. Ramirez-Pastor, T. P. Eggarter, V. D. Pereyra, and J. L. Riccardo, Phys. Rev. B **59**, 11027 (1999).
[20] A. J. Ramirez-Pastor, J. L. Riccardo, and V. D. Pereyra, Surf. Sci. **411**, 294 (1998); Langmuir **16**, 10169 (2000).
[21] F. Romá, A. J. Ramirez-Pastor, and J. L. Riccardo, Langmuir **16**, 9406 (2000); J. Chem. Phys. **114**, 10932 (2001).
[22] F. Romá, A. J. Ramirez-Pastor, and J. L. Riccardo, Phys. Rev. B **68**, 205407 (2003).
[23] S. Iijima, Nature (London) **354**, 56 (1991).
[24] S. Iijima and T. Ichihashi, Nature (London) **363**, 603 (1993).
[25] D. S. Bethune, C. H. Kiamg, M. S. deVries, G. Gorman, R. Savoy, J. Vasquez, and R. Beyers, Nature (London) **363**, 605 (1993).
[26] P. M. Ajayan and S. Iijima, Nature (London) **361**, 333 (1993).
[27] E. Dujardin, T. W. Ebbesen, H. Hiura, and K. Tanigaki, Science **265**, 1850 (1994).
[28] C. Martin, J. P. Coulomb, Y. Grillet, and R. Kahn, *Fundamentals of Adsorption: Proceedings of the Fifth International Conference*, edited by M. D. LeVan (Kluwer Academic, Boston, MA, 1996), p. 587.
[29] C. Martin, N. Tosi-Pellenq, J. Patarin, and J. P. Coulomb, Langmuir **14**, 1774 (1998).
[30] A. D. Migone and S. Talapatra, in *Encyclopedia of Nanoscience and Nanotechnology*, edited by H. S. Nalwa (American Scientific, Los Angeles, CA, 2004), Vol. 4, p. 749.
[31] G. Stan, M. J. Bojan, S. Curtarolo, S. M. Gatica, and M. W. Cole, Phys. Rev. B **62**, 2173 (2000).
[32] T. Wilson, A. Tyburski, M. R. DePies, O. E. Vilches, D. Becquet, and M. Bienfait, J. Low Temp. Phys. **126**, 403 (2002).
[33] T. Wilson and O. E. Vilches, Low Temp. Phys. **29**, 732 (2003).
[34] N. M. Urban, S. M. Gatica, M. W. Cole, and J. L. Riccardo, Phys. Rev. B **71**, 245410 (2005).
[35] M. Bienfait, P. Zeppenfeld, N. Dupont-Pavlovsky, M. Muris, M. R. Johnson, T. Wilson, M. DePies, and O. E. Vilches, Phys. Rev. B **70**, 035410 (2004).
[36] M. M. Calbi, S. M. Gatica, M. J. Bojan, G. Stan, and M. W. Cole, Rev. Mod. Phys. **73**, 857 (2001).
[37] M. M. Calbi and J. L. Riccardo, Phys. Rev. Lett. **94**, 246103 (2005).
[38] R. A. Trasca, M. M. Calbi, and M. W. Cole, Phys. Rev. E **65**, 061607 (2002).
[39] R. A. Trasca, M. M. Calbi, M. W. Cole, and J. L. Riccardo, Phys. Rev. E **69**, 011605 (2004).
[40] L. Chen and J. K. Johnson, Phys. Rev. Lett. **94**, 125701 (2005).
[41] J. V. Pearce, M. A. Adams, O. E. Vilches, M. R. Johnson, and H. R. Glyde, Phys. Rev. Lett. **95**, 185302 (2005).
[42] L. Heroux, V. Krungleviciute, M. M. Calbi, and A. D. Migone, J. Phys. Chem. B **110**, 1297 (2006).
[43] S. M. Gatica, M. J. Bojan, G. Stan, and M. W. Cole, J. Chem. Phys. **114**, 3765 (2001).
[44] W. Shi and K. J. Johnson, Phys. Rev. Lett. **91**, 015504 (2003).
[45] A. Kuznetsova, J. T. Yates, Jr., J. Liu, and R. E. Smalley, J. Chem. Phys. **112**, 9590 (2000).
[46] A. Kuznetsova, D. B. Mawhinney, V. Naumenko, J. T. Yates, Jr.,J. Liu, and R. E. Smalley, Chem. Phys. Lett. **321**, 292 (2000).
[47] M. W. Cole, V. H. Crespi, G. Stan, C. Ebner, J. M. Hartman, S. Moroni, and M. Boninsegni, Phys. Rev. Lett. **84**, 3883 (2000).
[48] w_T could account for the lateral interaction energy between two atoms adsorbed in (1) parallel neighbor lines formed inside a single nanotube, (2) neighbor interstitial lines, or (3) parallel neighbor lines formed on the external surface of a nanotube bundle.
[49] L. Onsager, Phys. Rev. **65**, 117 (1944).
[50] G. F. Newell and E. W. Montroll, Rev. Mod. Phys. **25**, 353 (1953).
[51] T. L. Hill, *An Introduction to Statistical Thermodynamics* (Addison-Wesley, Reading, MA. 1960).
[52] M. Schick, J. S. Walker, and M. Wortis, Phys. Lett. **58**, 479 (1976).
[53] M. Schick, J. S. Walker, and M. Wortis, Phys. Rev. B **16**, 2205 (1977).
[54] C. E. Campbell and M. Schick, Phys. Rev. A **5**, 1919 (1972).

[55] D. P. Landau, Phys. Rev. B **27**, 5604 (1983).
[56] R. B. Griffiths, Phys. Rev. **136**, A437 (1964).
[57] R. B. Griffiths, J. Math. Phys. **8**, 478 (1967); J. Chem. Phys. **8**, 484 (1967).
[58] C-Y. Weng, R. B. Griffiths, and M. E. Fisher, Phys. Rev. **162**, 475 (1967).
[59] M. E. Fisher, Phys. Rev. **162**, 480 (1967).
[60] P. M. Pasinetti, J. L. Riccardo, and A. J. Ramirez-Pastor, J. Chem. Phys. **122**, 154708 (2005).
[61] P. M. Pasinetti, J. L. Riccardo, and A. J. Ramirez-Pastor, Physica A **355**, 383 (2005).
[62] K. Hukushima and K. Nemoto, J. Phys. Soc. Jpn. **65**, 1604 (1996).
[63] D. J. Earl and M. W. Deem, Phys. Chem. Chem. Phys. **7**, 3910 (2005).
[64] M. E. Fisher, in *Critical Phenomena*, edited by M. S. Green (Academic, London, 1971), p. 1.
[65] V. Privman, *Finite Size Scaling and Numerical Simulation of Statistical Systems* (World Scientific, Singapore, 1990).
[66] K. Binder, *Applications of the Monte Carlo Method in Statistical Physics: Topics in Current Physics* (Springer, Berlin, 1984), Vol. 36.
[67] D. Nicholson and N. G. Parsonage, *Computer Simulation and the Statistical Mechanics of Adsorption* (Academic, London, 1982).
[68] N. Metropolis, A. W. Rosenbluth, M. N. Rosenbluth, A. H. Teller, and E. Teller, J. Chem. Phys. **21**, 1087 (1953).
[69] K. Kawasaki, in *Phase Transitions and Critical Phenomena*, edited by C. Domb and M. S. Green (Academic, London, 1972), Vol. 2.
[70] By inspecting Fig. 1, it is possible to note that the configuration presented in (a) was formed on the sublattice 1.
[71] B. D. Metcalf, Phys. Lett. A **45**, 1 (1973).
[72] W. Kinzel and M. Schick, Phys. Rev. B **23**, 3435 (1981).
[73] K. K. Chin and D. P. Landau, Phys. Rev. B **36**, 275 (1987).
[74] P. M. Pasinetti, F. Romá, J. L. Riccardo, and A. J. Ramirez-Pastor, Phys. Rev. B **74**, 155418 (2006).
[75] As it is common in MC simulations, one represents the system with a unit cell of sites that is repeated periodically. Then, the choice of appropriate sizes in the transverse direction has to be done in such a way that the ordered structures are not disturbed.
[76] E. Barouch, B. M. McCoy, and T. T. Wu, Phys. Rev. Lett. **31**, 1409 (1973).
[77] K. Binder and J. S. Wang, J. Stat. Phys. **55**, 87 (1989).
[78] A systematic analysis of critical exponents for each w_L/w_T was not carried out since this was out of the scope of the present work.
[79] The calculations for $w_L/w_T=1.0$ and $w_L/w_T=-1.0$ were carried out with an effort reaching almost the limits of our computational capabilities. In the case of intermediate values of w_L/w_T, the number of MCS was restricted in order to get results in a reasonably computational time. These conditions are reflected in the different values of the numerical errors reported in Table II.